Multiband Superconductivity with Unexpected Deficiency of Nodal Quasiparticles in $CeCu_2Si_2$

Shunichiro Kittaka,[1] Yuya Aoki,[1] Yasuyuki Shimura,[1] Toshiro Sakakibara,[1] Silvia Seiro,[2] Christoph Geibel,[2] Frank Steglich,[2] Hiroaki Ikeda,[3] and Kazushige Machida[4]

[1]*Institute for Solid State Physics (ISSP), University of Tokyo, Kashiwa, Chiba 277-8581, Japan*

[2]*Max Planck Institute for Chemical Physics of Solids, 01187 Dresden, Germany*

[3]*Department of Physics, Kyoto University, Kyoto 606-8502, Japan*

[4]*Department of Physics, Okayama University, Okayama 700-8530, Japan*

(Received 28 June 2013; published 12 February 2014)

Superconductivity in the heavy-fermion compound $CeCu_2Si_2$ is a prototypical example of Cooper pairs formed by strongly correlated electrons. For more than 30 years, it has been believed to arise from nodal d-wave pairing mediated by a magnetic glue. Here, we report a detailed study of the specific heat and magnetization at low temperatures for a high-quality single crystal. Unexpectedly, the specific-heat measurements exhibit exponential decay with a two-gap feature in its temperature dependence, along with a linear dependence as a function of magnetic field and the absence of oscillations in the field angle, reminiscent of multiband full-gap superconductivity. In addition, we find anomalous behavior at high fields, attributed to a strong Pauli paramagnetic effect. A low quasiparticle density of states at low energies with a multiband Fermi-surface topology would open a new door into electron pairing in $CeCu_2Si_2$.

DOI: 10.1103/PhysRevLett.112.067002 PACS numbers: 74.70.Tx, 74.25.Bt, 74.25.Op

After the first discovery of heavy-fermion superconductivity in $CeCu_2Si_2$ [1], a number of unconventional superconductors, such as high-T_c cuprates, iron-pnictides, organic, and heavy-fermion superconductors, have been found. Among the various issues on these novel superconductors, the identification of the superconducting gap structure is one of the most important subjects because it is closely related to the pairing mechanism. Particularly, the gap symmetry of $CeCu_2Si_2$ has attracted attention because superconductivity in this compound emerges near an antiferromagnetic (AFM) quantum critical point and heavy quasiparticles (QPs) couple to quantum critical spin excitations [2].

Up to now, the gap symmetry of $CeCu_2Si_2$ was inferred to be an even-parity d-wave type with line nodes. The well resolved decrease in the NMR Knight shift below the transition temperature $T_c \simeq 0.6$ K [3] is a strong evidence for the spin part of the Cooper pairs being a singlet. Indeed, the low-T saturation of the upper critical field H_{c2} is attributed to the Pauli paramagnetic effect due to the spin-singlet pairing. Based on the T^3 dependence of the nuclear relaxation rate $1/T_1$ and the absence of a coherence peak [4–6], the superconducting gap was proposed to possess line nodes. Presently the debate is whether the gap symmetry is $d_{x^2-y^2}$ or d_{xy} type [7,8]. However, the presence of line nodes as well as the symmetry of the gap has not yet been studied precisely using low-T thermodynamic properties.

To elucidate the gap structure of $CeCu_2Si_2$, the specific heat C in magnetic fields H is herein measured at temperatures down to 40 mK using a high-quality single-crystalline sample. Measurement of C probes the QP density of states (DOS) that depends on the nodal structure. An S-type single crystal (having a mass of 13.8 mg) was used that presents only a superconducting ground state without magnetic ordering, since other types of $CeCu_2Si_2$ show additional contributions in $C(T)$ at low temperatures that make the interpretation of the data difficult. Growth and characterization of the single crystal is described in Ref. [9]. The specific heat was measured by the standard quasi-adiabatic heat-pulse method. The dc magnetization was measured using a high-resolution capacitive Faraday magnetometer with a vertical field gradient of 5 T/m. All the measurements were done at ISSP.

Figure 1(a) plots the T dependence of the nuclear-subtracted specific heat $C_e = C - C_n$ divided by T, measured with various fields applied along the [100] axis [as explained in Supplemental Material [10] (I)]. In the normal state, C_e/T gradually increases upon cooling. This non-Fermi-liquid behavior arises from three-dimensional spin-density-wave fluctuations occurring in the vicinity of an AFM quantum critical point [11,12].

Consider the zero-field data. Although $T_c = 0.6$ K is slightly lower than the optimum value for this compound (~0.65 K), the sample shows a lower residual DOS at the base temperature and a sharper transition at T_c than those of previous reports [12,13]. These facts indicate the high quality of the present sample with no significant impurities. The specific-heat jump at T_c is found to be $\Delta C_e(T_c)/\gamma T_c \sim 1.2$, slightly smaller than the weak-coupling BCS prediction of 1.43. At intermediate temperatures, C_e/T exhibits a nearly linear T dependence that is consistent with the T^3 dependence of $1/T_1$ observed down to 0.1 K [4–6].

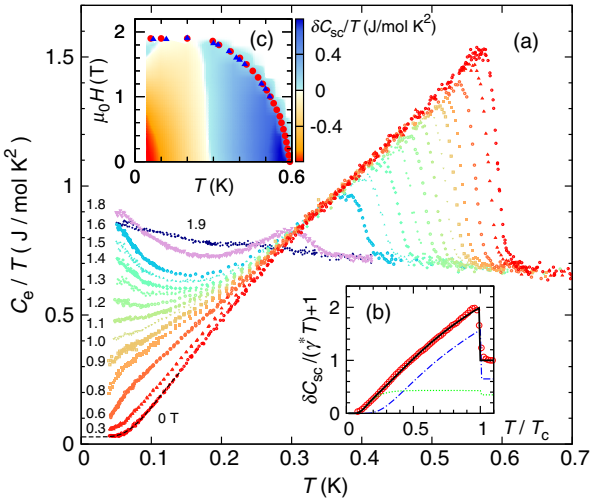

FIG. 1 (color online). (a) Electronic specific heat of an S-type $CeCu_2Si_2$ single crystal divided by temperature, C_e/T, as a function of T measured in $H\|[100]$. The dashed line is a fit to the low-T part of the $C_e(T)$ data at 0 T using the BCS formula $C_e(T) = A\exp(-\Delta_0/T) + \gamma_0 T$. (b) Temperature variation of $\delta C_{sc}(T,H)/\gamma^* T + 1$ at $H = 0$ and a best fit to the two-gap BCS model (solid line). Here, $\delta C_{sc}(T,H) = C_e(T,H) - C_e(T, 3\text{ T})$ and $\gamma^* = 0.84$ J/(mol K^2) are introduced to satisfy entropy balance in the BCS framework. The gradual increase of the normal-state C_e/T upon cooling is included in $\delta C_{sc}(T,H)$. The contribution of each gap to the total specific heat is also shown. (c) Field-temperature phase diagram for $H\|[100]$ determined by the specific-heat (circles) and magnetization (triangles) measurements. A contour plot of $\delta C_{sc}(T,H)/T$ in the superconducting state is shown using the data from (a). Anomalous $\delta C_{sc} > 0$ behavior that can be ascribed to the Pauli paramagnetic effect is clearly seen in the high-H and low-T region below 0.1 K.

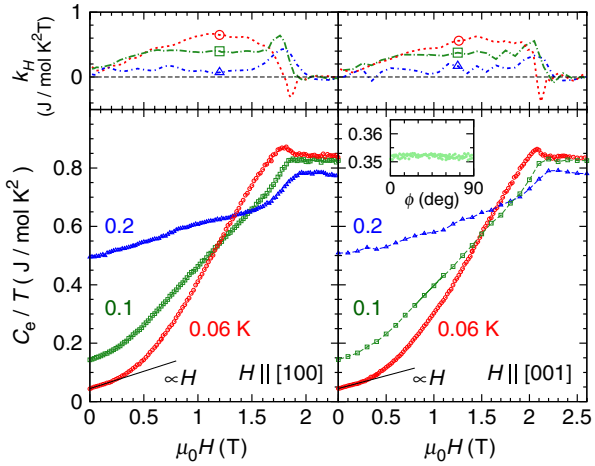

FIG. 2 (color online). The ratio C_e/T and its slope $k_H = d(C_e/T)/d(\mu_0 H)$ as a function of magnetic field applied parallel to the [100] and [001] directions at 0.06 (circles), 0.1 (squares), and 0.2 K (triangles). No hysteresis is found with increasing and decreasing fields. Inset shows $C_e/T(\phi)$ at 0.1 K in 0.7 T.

At lower temperatures, however, C_e/T shows a large positive curvature, in contrast to the linear behavior predicted for a line-node gap [see Supplemental Material [10] (II)]. The data can be fit using the BCS function $C_e = A\exp(-\Delta_0/T) + \gamma_0 T$ with $\Delta_0 = 0.39$ K and $\gamma_0 = 0.028$ J/(mol K^2) [dashed line in Fig. 1(a)]. Comparison with previous results [12] shows that this positive curvature is insensitive to sample quality, i.e., to a change in γ_0 in the range 0.01 to 0.08 J/(mol K^2), which would originate from nonsuperconducting inclusions in the sample. Therefore, its origin cannot be attributed to the impurity-scattering effect of line-node superconductors [14]. Furthermore, extrapolating the linear behavior in $C(T)/T$ versus T observed in the range 80 mK $\le T \le$ 250 mK to $T = 0$ results in a negative intercept, not only for the present data, but for all published S-type samples (e.g., Ref. [12]). This implies the crossover to a high power law below 80 mK, proving the intrinsic QP DOS at low energy to be extremely small in $CeCu_2Si_2$.

On the basis of a phenomenological two-gap model within the conventional BCS framework [15], the T dependence of C_e/T including the linear behavior in the intermediate-T region can be reproduced [Fig. 1(b)] using two BCS gaps, $\Delta_1/k_B T_c = 1.76$ and $\Delta_2/k_B T_c = 0.7$, whose weights are 65% and 35% of the total DOS, respectively. A signature of multiband superconductivity is found in the dependence of C_e/T with H as well: C_e/T at 0.6 T shows a kink at 65 mK and decreases rapidly with cooling. The T variation of C_e/T matches with the prediction of two-gap superconductivity in the absence of nodal QPs. Furthermore, the T^3-like dependence of $1/T_1$ down to $\sim 0.2 T_c$ is naturally led by the multiband full-gap model, as is demonstrated for the iron-pnictide superconductors [16]; $1/T_1$ measurement below 100 mK is desired to further confirm a fully opened multigap.

Direct evidence for the deficiency of nodal QP excitations comes from the field variation of $C_e(H)$ at 60 mK. For both field orientations parallel and perpendicular to the [001] axis, C_e gradually increases in proportion to H for fields up to about 0.2 T (Fig. 2), in contrast to the $\sqrt{H}$ variation of $C_e(H)$ for nodal superconductors [17]. The upward curvature at 0.5 T is ascribed to the abrupt enhancement of QP DOS due to the minor gap. Because the magnetic field quickly exceeds the lower critical value of a few millitesla [18], the sample is in the vortex state. According to calculations based on microscopic quasiclassical theory [19,20], the initial slope of $C_e(H)$ in the vortex state is $dC_e/dH|_{H\sim 0} = [C_e(H_{c2}) - C_e(0)]/(\alpha H_{c2}^{orb})$ where H_{c2}^{orb} is the orbital-limiting field. The parameter α depends on the gap structure, and has a maximum value of 0.8 for an isotropic gap. A minor gap or a gap anisotropy decreases the value of α, eventually approaching zero for a nodal gap. Using this relation, with $\mu_0 H_{c2}^{orb} = 10$ T estimated from $H_{c2}^{orb} \sim 0.7 T_c dH_{c2}/dT|_{T_c}$ from Fig. 1(c), one obtains $\alpha \sim 0.67$ from the $C_e(H)$ data at 60 mK for $H\|[100]$. This intermediate value of α favors weakly anisotropic or multiband full-gap superconductivity.

To search for the vertical line nodes, $C_e(\phi)$ is measured by rotating the field within the ab plane [see inset of Fig. 2 and Supplemental Material [10] (III)], where ϕ is the azimuthal angle between H and the crystal [100] axis. Doppler-shift analyses predict that, for a rotating magnetic field, the QP DOS will oscillate and exhibit local minima when H is along the nodal or gap-minimum directions [21,22]. For example, $C_e(\phi)$ for the $d_{x^2-y^2}$-wave superconductor $CeIrIn_5$ (with $T_c = 0.4$ K) has a fourfold oscillation with a large A_4 value of 2% [23], where A_4 is the amplitude normalized by the field dependent part of the specific heat $C_H = C_e(H) - C_e(0)$. In contrast to $CeIrIn_5$, no angular oscillation of $C_e(\phi)$ is observed for $CeCu_2Si_2$ at a temperature of 0.1 (0.2) K within the 0.1% (0.5%) sensitivity of the measurements of A_4. This result implies that QPs are induced by H isotropically with respect to ϕ, so that vertical line nodes are not detected for $C_e(\phi)$. Possible $C_e(\phi)$ oscillation due to the in-plane H_{c2} anisotropy [7] was not detected within the present experimental accuracy.

Based on the present results, $CeCu_2Si_2$ is a "nodeless" multiband superconductor. Because $C_e(T, H, \phi)$ is sensitive to the contribution from heavy QPs, "nodeless" implies that the gap is fully open in the heavy-mass bands. To get an insight into the band structure of $CeCu_2Si_2$, first-principles calculations were performed [see Supplemental Material [10] (IV)]. There are a flat electron band around the X point with the heaviest mass and two hole bands around the Z point [Figs. 3(a)–(c)]. The heavy electron band resembles

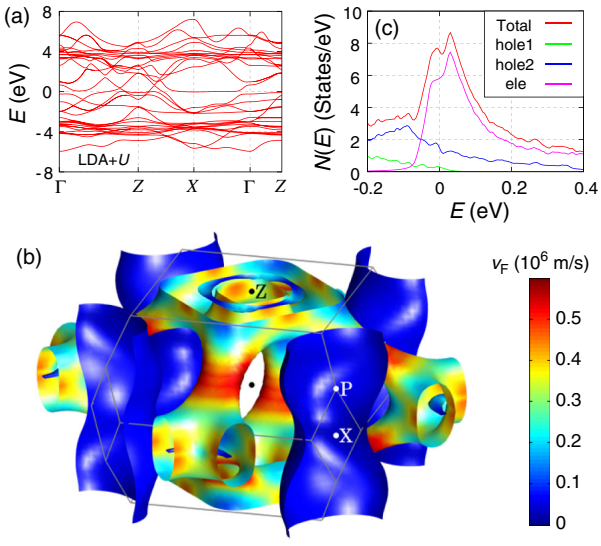

FIG. 3 (color online). (a) Band structure of $CeCu_2Si_2$ calculated using the LDA + U method. (b) The calculated Fermi surfaces colored by the magnitude of the Fermi velocity v_F. (c) The total density of states and the partial density of states for the three bands. The Fermi level corresponds to $E = 0$. Here "hole1" and "hole2" are a small hole ring and a connected hole sheet located around the Z point, respectively, and "ele" is a tubular electron sheet located around the X point.

the one obtained in previous studies [8,24] and its flat parts are connected by the nesting vector $\boldsymbol{Q} = (0.215, 0.215, 1.458)$ around which magnetic excitations have been observed in inelastic neutron experiments [2].

In this Fermi-surface topology, the results rule out a $d_{x^2-y^2}$-wave state. It has line nodes on the electron Fermi sheet of heavy mass, which is incompatible with "nodeless" superconductivity. Likewise, realization of an ordinary d_{xy}-wave state would require quite unusual situations such that the effective mass of the hole band is negligibly small so that the nodal structure cannot be detected by the $C(T, H)$ measurements. Otherwise, we have to seek possibilities of fully-gapped states instead of a nodal d-wave state, including an unconventional s-wave, such as $s_{\pm}$-wave [25], a conventional s-wave, or a fully-gapped $d + id$ state. Indeed, the two-gap structure detected in the $C_e(T, H)$ measurements indicates that the mass of the hole bands is not negligible. Nevertheless, fully-gapped states apparently contradict some key experiments that point to nodal d-wave symmetry, such as the spin resonance observed in neutron scattering [2]. Therefore, there might remain a possibility of nodal d-wave superconductivity, e.g., with a very unusual evolution of the gap size near the nodes, leading to a small DOS at low energies. Further investigations are needed to explain this discrepancy.

In addition to multiband superconductivity with unexpectedly small QP excitations, the specific-heat measurements reveal unusual phenomena at high fields. Above 1.2 T, a remarkable upturn is observed in the T variation of C_e/T when cooled below 0.15 K. This upturn disappears when H reaches H_{c2}, indicating that the phenomenon is related to superconductivity. Strikingly, C_e/T at 1.8 T exceeds the normal-state value when $T \leq 80$ mK [Figs. 1(a), 1(c), and 2] in spite of the presence of a distinct superconducting transition at a higher temperature of about 0.35 K. These anomalous features cannot be attributed to the nuclear Schottky contribution that increases in proportion to H^2. Qualitatively the same behavior is observed for the $H \| [001]$ direction as well.

To further investigate this strange high-field behavior, the dc magnetization $M(T, H)$ is measured down to 70 mK for $H \| [100]$ using the same sample. At 70 mK, the hysteresis loop of $M(H)$ is small except at low fields [Fig. 4(a)]. This result verifies the purity of the sample. A diamagnetic contribution can be observed up to 1.9 T, implying that the sample remains superconducting even when C_e/T exceeds its normal-state value. Nevertheless, the diamagnetic contribution in the range 1.8 T $\lesssim \mu_0 H \leq$ 1.9 T is unusually suppressed upon cooling below 0.12 K [Figs. 4(b) and 4(c)], suggesting a strong pair-breaking effect near H_{c2}. Indeed, a kink develops in $M(H)$ at H_{c2} when cooled, attributed to a strong Pauli paramagnetic effect [26,27]. This effect is also evident in $C_e(H)$ for $T = 0.1$ and 0.2 K. The slope of $C_e(H)$, i.e., $k_H = d(C_e/T)/d(\mu_0 H)$, is enhanced as H approaches

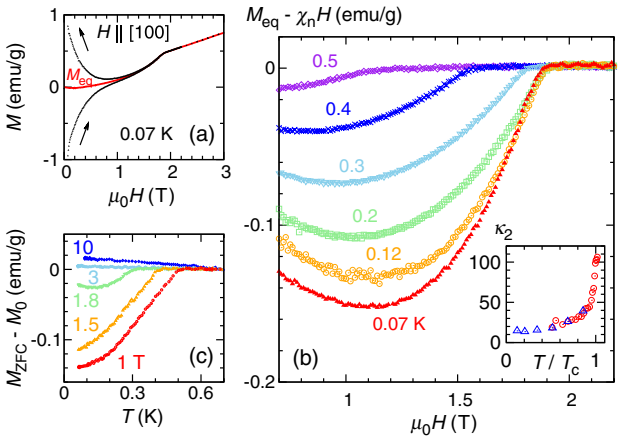

FIG. 4 (color online). (a) Magnetization M of $CeCu_2Si_2$ in $H\|[100]$ at 70 mK. The solid line represents the equilibrium magnetization M_{eq} obtained by averaging over increasing and decreasing field sweeps. (b) Graphs of $M_{eq}-\chi_n H$ at 0.07, 0.12, 0.2, 0.3, 0.4, and 0.5 K, where $\chi_n H$ is the paramagnetic contribution. The inset shows temperature dependence of the Maki parameter κ_2 evaluated from the specific-heat (circles) and the magnetization (triangles) using the relations $d(M_{eq}-\chi_n H)/dH|_{H_{c2}} = 1/4\pi\beta(2\kappa_2^2-1)$ and $(\Delta C/T)|_{T_c} = (dH_{c2}/dT)^2/4\pi\beta(2\kappa_2^2-1)$. Here, ΔC is the jump in the specific heat at $T_c(H)$ from Fig. 1(a). The value $\beta = 1.16$ assumes a triangular vortex lattice. The slope of dH_{c2}/dT is estimated using the data in Fig. 1(c). (c) Magnetization measured during a zero-field cooling process, M_{ZFC}, at 1, 1.5, 1.8, 3, and 10 T after subtracting the value M_0 of M_{ZFC} at 0.7 K.

H_{c2} (Fig. 2), although the behavior is hidden at 60 mK by the anomalous C_e/T upturn in the high-field state. The Maki parameter κ_2 shows a large decrease on cooling near T_c [inset of Fig. 4(b)], in good agreement with theory for strongly Pauli-limited superconductors. It is concluded that the unusual high-field behavior can be ascribed to a strong paramagnetic depairing effect.

For a clean superconductor with a strong paramagnetic effect, the superconducting-to-normal phase transition is expected to change from second to first order at low temperatures [28]. However, the transition at H_{c2} oddly remains second order in $CeCu_2Si_2$, indicated by a continuous change of $M(H)$ across H_{c2} without hysteresis and a leveling off of κ_2 at low temperatures. These features cannot be explained simply by the paramagnetic effect for single-band superconductivity.

Returning to the T variation of C_e/T in Fig. 1(a), it can be shown that its unusual high-field behavior is related to the energy dependence of the total DOS. In general,

$$C_e/T = \int x^2 N(xT)/[4\cosh^2(x/2)]dx, \qquad (1)$$

where $N(E)$ is the energy dependence of the total DOS and the energy E is replaced with xT. By approximating $N(E) = a|E|^n$, which is valid near $E \sim 0$, Eq. (1) can be rewritten as $C_e/T = a'N(T)$, where a, n, and a' are constants. This relationship demonstrates that the T dependence of C_e/T at low temperatures mimics $N(E)$ at low energies.

In this context, the T variation in C_e/T at each field can be understood by taking into account the presence of two gaps as well as the strong paramagnetic effect. Theory predicts that $N(E)$ has a V-shaped structure in the vortex state [29], i.e., $N(E) \propto |E|$ near $E \sim 0$ with an edge-singularity peak at $|E| \sim \Delta$. The observed kink in C_e/T at low H, such as at 0.6 T, is ascribed to the edge singularity of the small V-shaped DOS of a minor gap superposed on the large V-shaped DOS of a major gap. At higher fields, assuming the strong paramagnetic effect holds for the minor gap, the edge singularity is shifted toward lower energy [26] and an upturn in C_e/T corresponding to the tail of the singularity in the high-energy side is observed. Because the V-shaped DOS of the major gap gradually approaches the normal-state DOS with increasing field, C_e/T can exceed the normal-state value near H_{c2} if the DOS enhancement due to the edge singularity of the minor gap remains prominent. The upward curvature in $C_e(H)$ near 0.5 T is a sign of the paramagnetic effect for the minor gap. While these analyses suggest that the two-band full-gap model, in the presence of a strong paramagnetic effect, can explain the anomalous $C_e(T,H)$ behavior satisfactorily, there remain other possible origins, such as the occurrence of an AFM ordering in the high-field superconducting state. To further confirm the Pauli-limited two-gap scenario, detailed calculations of $C(T,H)$ based on the microscopic theory are in progress [30].

In summary, we have investigated the low-temperature specific heat and magnetization of a high-quality S-type single crystal of $CeCu_2Si_2$. Our study has provided thermodynamic evidence for multiband superconductivity, an unexpected deficiency of nodal QP excitations, and a strong Pauli paramagnetic effect in $CeCu_2Si_2$. The discovery of unexpectedly small QP DOS at low energies challenges the long-held view of this heavy-fermion superconductor whose pairing symmetry is believed to be of the nodal d-wave type. These findings help resolve long-standing issues about the pairing mechanism in $CeCu_2Si_2$.

We acknowledge helpful discussions with Y. Kitaoka. We also thank Y. Tsutsumi for supporting the calculation on the basis of the two-gap model. H. I. thanks M.-T. Suzuki for assistance with the LDA + U calculations. This work was supported by a Grants-in-Aid for Scientific Research on Innovative Areas "Heavy Electrons" (No. 20102007, No. 23102705) from MEXT, and KAKENHI (No. 25800186, No. 24340075, No. 21340103, No. 23340095, No. 24540369) from JSPS.

[1] F. Steglich, J. Aarts, C. D. Bredl, W. Lieke, D. Meschede, W. Franz, and H. Schäfer, Phys. Rev. Lett. **43**, 1892 (1979).
[2] O. Stockert, J. Arndt, E. Faulhaber, C. Geibel, H. S. Jeevan, S. Kirchner, M. Loewenhaupt, K. Schmalzl, W. Schmidt, Q. Si, and F. Steglich, Nat. Phys. **7**, 119 (2011).

[3] K. Ueda, Y. Kitaoka, H. Yamada, Y. Kohori, T. Kohara, and K. Asayama, J. Phys. Soc. Jpn. **56**, 867 (1987).
[4] Y. Kitaoka, K. Ueda, K. Fujiwara, H. Arimoto, H. Iida, and K. Asayama, J. Phys. Soc. Jpn. **55**, 723 (1986).
[5] K. Ishida, Y. Kawasaki, K. Tabuchi, K. Kashima, Y. Kitaoka, K. Asayama, C. Geibel, and F. Steglich, Phys. Rev. Lett. **82**, 5353 (1999).
[6] K. Fujiwara, Y. Hata, K. Kobayashi, K. Miyoshi, J. Takeuchi, Y. Shimaoka, H. Kotegawa, T. C. Kobayashi, C. Geibel, and F. Steglich, J. Phys. Soc. Jpn. **77**, 123711 (2008).
[7] H. A. Vieyra, N. Oeschler, S. Seiro, H. S. Jeevan, C. Geibel, D. Parker, and F. Steglich, Phys. Rev. Lett. **106**, 207001 (2011).
[8] I. Eremin, G. Zwicknagl, P. Thalmeier, and P. Fulde, Phys. Rev. Lett. **101**, 187001 (2008).
[9] S. Seiro, M. Deppe, H. Jeevan, U. Burkhardt, and C. Geibel, Phys. Status Solidi B **247**, 614 (2010).
[10] See Supplemental Material at http://link.aps.org/supplemental/10.1103/PhysRevLett.112.067002 for the analyses of the specific-heat data, the results of field-angle-resolved specific-heat measurements and the method of the band structure calculation.
[11] P. Gegenwart, C. Langhammer, C. Geibel, R. Helfrich, M. Lang, G. Sparn, F. Steglich, R. Horn, L. Donnevert, A. Link, and W. Assmus, Phys. Rev. Lett. **81**, 1501 (1998).
[12] J. Arndt, O. Stockert, K. Schmalzl, E. Faulhaber, H. S. Jeevan, C. Geibel, W. Schmidt, M. Loewenhaupt, and F. Steglich, Phys. Rev. Lett. **106**, 246401 (2011).
[13] C. D. Bredl, H. Spille, U. Rauchschwalbe, W. Lieke, F. Steglich, G. Cordier, W. Assmus, M. Herrmann, and J. Aarts, J. Magn. Magn. Mater. **31–34**, 373 (1983).
[14] C. Kübert and P. J. Hirschfeld, Solid State Commun. **105**, 459 (1998).
[15] F. Bouquet, Y. Wang, R. A. Fisher, D. G. Hinks, J. D. Jorgensen, A. Junod, and N. E. Phillips, Europhys. Lett. **56**, 856 (2001).
[16] M. Yashima, H. Nishimura, H. Mukuda, Y. Kitaoka, K. Miyazawa, P. M. Shirage, K. Kihou, H. Kito, H. Eisaki, and A. Iyo, J. Phys. Soc. Jpn. **78**, 103702 (2009).
[17] G. E. Volovik, JETP Lett. **58**, 469 (1993).
[18] U. Rauchschwalbe, W. Lieke, C. D. Bredl, F. Steglich, J. Aarts, K. M. Martini, and A. C. Mota, Phys. Rev. Lett. **49**, 1448 (1982).
[19] N. Nakai, M. Ichioka, and K. Machida, J. Phys. Soc. Jpn. **71**, 23 (2002).
[20] N. Nakai, P. Miranović, M. Ichioka, and K. Machida, Phys. Rev. B **70**, 100503 (2004).
[21] I. Vekhter, P. J. Hirschfeld, J. P. Carbotte, and E. J. Nicol, Phys. Rev. B **59**, R9023 (1999).
[22] T. Sakakibara, A. Yamada, J. Custers, K. Yano, T. Tayama, H. Aoki, and K. Machida, J. Phys. Soc. Jpn. **76**, 051004 (2007).
[23] S. Kittaka, Y. Aoki, T. Sakakibara, A. Sakai, S. Nakatsuji, Y. Tsutsumi, M. Ichioka, and K. Machida, Phys. Rev. B **85**, 060505 (2012).
[24] G. Zwicknagl and U. Pulst, Physica (Amsterdam) **B186–188**, 895 (1993).
[25] K. Kuroki, S. Onari, R. Arita, H. Usui, Y. Tanaka, H. Kontani, and H. Aoki, Phys. Rev. Lett. **101**, 087004 (2008).
[26] M. Ichioka and K. Machida, Phys. Rev. B **76**, 064502 (2007).
[27] K. Machida and M. Ichioka, Phys. Rev. B **77**, 184515 (2008).
[28] Y. Matsuda and H. Shimahara, J. Phys. Soc. Jpn. **76**, 051005 (2007), and references therein.
[29] N. Nakai, P. Miranović, M. Ichioka, and K. Machida, Phys. Rev. B **73**, 172501 (2006).
[30] Y. Tsutsumi, M. Ichioka, and K. Machida, in preparation.